Uncertainty quantification of kinetic models using adjoint-driven active subspace algorithms

Ahmed Hassan, Moataz Sabry, Vincent Le Chenadec, Taraneh Sayadi

HAL Id: hal-03852538
https://hal.science/hal-03852538

Submitted on 15 Nov 2022

Uncertainty quantification of kinetic models using adjoint-driven active subspace algorithms

Ahmed Hassan[a,*], Moataz Sabry[a], Vincent Le Chenadec[b], Taraneh Sayadi[a,c]

[a] *Institute for Combustion Technology, RWTH-Aachen University, Aachen, Germany*
[b] *Laboratoire Modélisation et Simulation Multi-Echelle, Université Gustave Eiffel, Champs-sur-Marne, France*
[c] *Institut Jean-le-Rond d'Alembert, CNRS/Sorbonne Université, Paris, France*

Abstract

Keywords: Kinetic models; Uncertainty quantification; Active subspaces; Adjoint-based methods

1. Introduction

Computational simulations of chemically reacting flows leverage a wide range of components to account for the kinetics of the combustion processes, the thermodynamics of the interacting compounds as well as their transport properties. Their predictability is particularly sensitive to the kinetic models, which come in different flavors depending on the level of fidelity employed. These models in turn include a large number of parameters, subject to uncertainties that are essential to quantify in order to assess the applicability and performance of the underlying models.

Monte Carlo methods have traditionally been applied to assess the existing model uncertainties. However, their slow convergence and high computational cost have given rise to alternative approaches that reduce the cost by considering a smaller set of the parameter space. Some of these approaches include probabilistic methods such as Polynomial Chaos Expansion (PCE) [1] and related methods [2, 3] applicable to high-dimensional parameter spaces, and Gaussian process approximation method (Kriging) [4]. In most of these approaches, a response surface is formed from function evaluations (computationally intensive unsteady simulations) at sparsely and carefully selected points to approximate the dependence between the model parameters (input) and the quantity of interest (output). In the combustion community, the large number of parameters has motivated the development of various techniques to further speed up the construction of the response surfaces, some based on sensitivity analysis [5], High Dimensional Model Representations (HDMR) [6] and Artificial Neural Networks (ANN) [7]. A comprehensive review of response surface methods in the context of combustion simulations can be found elsewhere [8].

While effective in their own rights, most of these methods suffer from the curse of dimensionality and are not applicable as the number of parameters increases beyond a certain threshold, which is the case when considering detailed kinetic models of interest to this study. Some remedies include resorting to sensitivity analysis in order to lower the dimension of the parameter space. These methods can be divided into local and global alternatives. In local estimation methods, the parameter space is reduced based on the local estimations of the gradient; these methods therefore suffer from shortcomings such as sensitivity to noise. Global methods provide more robust sensitivity estimates, at a significant additional cost however [9, 10]. Alternatively, in the case of PCE, collocation techniques with sparse quadrature or adaptive regression strategies [11, 12] have been used to reduce the high-dimensional parameter space when constructing the response surface. These methods mainly rank the coordinates of the inputs. However, some models may vary most prominently along directions of the input space that are not aligned with the coordinate system.

Therefore, in this study, we adopt a different strategy, namely the Active Subspace Method (ASM) [9], where gradient information is used to detect and exploit the directions of the strongest variability of a given function to construct an approximation on a low-dimensional subspace of the function's inputs. ASM has successfully been applied to analyze the chemical kinetic uncertainty for liftoff height in a turbulent combustion application [13]. In a later work, Ji *et al.* [14] develop a method to simultaneously approximate the marginal PDFs of multiple quantities of interest, in particular, Ignition Delay Time (IDT) in an isobaric reactor and Laminar Flame Speed (LFS), based in both cases on the identification of a single active direction. In a recent work, Su *et al.* [15] have also employed active subspace method together with sensitivity analysis to identify extreme low-dimensional active subspace of the input parameter space of a dimethyl ether (DME) mechanism.

Using ASM, a certain number of gradient evaluations at distinct sample points in the input parameter space are required to obtain good estimates of the dominant directions. These gradients are usually estimated by either finite differences or local linear fitting, and the cost of their evaluation increases linearly with the number of parameters. In this work, we leverage the adjoint method [16] to compute gradient information at a cost comparable to a single function evaluation. Furthermore, the adjoint method is also used to provide a linear approximation of uncertainties in the active direction (LAAM). To the best knowledge of the authors, LAAM has never been applied to analyse uncertainties of chemical reaction networks, and in this respect this manuscript shows one of its first applications. We show that LAAM is an accurate way of defining uncertainties for this problem with a much lower cost, making this method a practical tool for extracting uncertainties, especially useful for large mechanisms. Cases are also considered where a single dominant direction can not be identified and a strategy is provided in order to include multiple active directions in the analysis. Finally, the limitations of the LAAM approach are presented and discussed.

The paper is organized as follows: Sec. 2 describes the methodologies for extracting the gradient and constructing the response surface using the active subspace algorithm. The described methods are then applied to three different cases in Sec. 3, extracting uncertainties with respect to model parameters and initial conditions, and their applicability and limitations are discussed. The conclusions and outlook of this work are then presented in Sec. 4.

2. Methodology

In this section, the algorithms for extracting the uncertainties and the relevant gradient information from the system of interest are briefly presented. The objective function of interest to this work is the ignition delay time (IDT), which is defined as the moment where the gradient of temperature reaches its maximal

value,

$$\text{IDT} = \underset{t_0 \leq t \leq t_f}{\arg\max} \dot{T}(t) \qquad (1)$$

where t_0 and t_f denotes the initial and final times. The system of interest consists of a zero-dimensional isochoric adiabatic reactor, the composition and temperature of which evolve according to

$$\begin{cases} \dfrac{\partial Y_i}{\partial t} = \dfrac{1}{\rho}\dot{\omega}_i \\[2mm] \dfrac{\partial T}{\partial t} = \dfrac{1}{\rho C_v}\dot{\omega}_T \end{cases} \qquad (2)$$

where (Y_i) $(i \in [\![1, N_s]\!])$ denote the species mass fractions, and C_v and ρ the mixture's average heat capacity at constant volume and density, respectively. The terms $(\dot{\omega}_i)$ denote the species' rates of consumption or production, which are related to the reaction rates,

$$K_j = A_j T^{b_j} \exp\left(\dfrac{-E_j}{RT}\right), \qquad (3)$$

where $j = [\![1, N_r]\!]$. N_r denotes the mechanism's number of reactions, and (A_j), (b_j) and (E_j) the Arrhenius coefficients parameterizing reaction j. The source term $\dot{\omega}_T$ is the heat release rate given by

$$\dot{\omega}_T = -\sum_{i=1}^{N_s} \dot{\omega}_i u_i, \qquad (4)$$

where u_i denotes the internal energy of species i.

2.1. Adjoint Method

The adjoint method performs the computation of the gradient of output functionals (real-valued quantities of interest) at a cost comparable to a single function evaluation, regardless of the number of components (parameters of the model) [17]. While efficient the adjoint method offers less flexibility than forward sensitivities methods, such as the finite difference method, to tackle implicit functions such as Eq. 1. As a consequence, the following alternative objective function, proposed by [18], is employed,

$$\mathcal{J} \equiv \text{IDT} = \frac{1}{2t_f}\int_0^{t_f} (T(t) - T_s(t))^2 \, \mathrm{d}t. \qquad (5)$$

where t_f is the final time, T_s the shifted temperature profile, and $t_s = -t_r \times 10^{-2}$[18] the shifting time, proportional to the reaction characteristic time t_r, defined as,

$$t_r = \left[\max\left(\frac{\partial T}{\partial t}\right)\right]^{-1} (T_f - T_0) \qquad (6)$$

Forming the Lagrange multiplier [18], the adjoint equations can be extracted, resulting in $\forall i \in [\![1, N_s]\!]$

$$-\frac{\mathrm{d}\xi_i}{\mathrm{d}t} = \frac{\partial J}{\partial Y_i} + \xi_j \frac{\partial}{\partial Y_i}\left(\frac{1}{\rho}\dot{\omega}_j\right) + \phi\frac{\partial}{\partial Y_i}\left(\frac{1}{\rho C_v}\dot{\omega}_T\right),$$

$$-\frac{\partial \phi}{\partial t} = \frac{\partial J}{\partial T} + \phi\frac{\partial}{\partial T}\left(\frac{\dot{\omega}_T}{\rho C_v}\right) + \xi_i\frac{\partial}{\partial Y_i}\left(\frac{\dot{\omega}_i}{\rho}\right)$$
$$(7)$$

where ξ_i is the adjoint variable corresponding to the Y_i equation and ϕ to the temperature equation (details regarding the extraction of the adjoint equations are provided in [18]). In the latter equations, J is the integrand already included in the definition of $\mathcal{J}$, namely

$$J \equiv \frac{1}{2t_f}(T - T_s)^2. \qquad (8)$$

The adjoint equations are integrated backward in time from the following conditions,

$$\begin{cases} \xi_i(t_f) = 0, \quad \forall i \in [\![1, N_s]\!], \\[2mm] \phi(t_f) = 0. \end{cases} \qquad (9)$$

The component of gradient associated with a parameter g is then given as

$$\frac{\mathrm{d}\mathcal{J}}{\mathrm{d}g} = \int_{t_0}^{t_f}\left[\frac{\partial J}{\partial g} + \xi_j\frac{\partial}{\partial g}\left(\frac{\dot{\omega}_j}{\rho}\right)\right.$$
$$\left. + \phi\frac{\partial}{\partial g}\left(\frac{\dot{\omega}_T}{\rho C_v}\right)\right]\mathrm{d}t. \qquad (10)$$

Here, g may denote a kinetics parameter (such as a given A_i, $i \in [\![1, N_s]\!]$), a thermodynamics coefficient, or a component of the initial condition.

The linearisation of the primal source terms ($\dot{\omega}_i$, $\dot{\omega}_T$, etc.) and objective ($\mathcal{J}$) are performed using automatic differentiation [19]. The primal and adjoint equations are implemented in the open-source package `Apophis.jl`.

The comparison of the extracted sensitivities (gradient components) using automatic differentiation (AD), and complex step differentiation (CSD), an alternative method for extracting accurate gradients (for more information regarding CSD refer to [20]), are compared in Fig. 1 for GRI 3.0 mechanism [18]. The agreement between the two approaches validates the adjoint method in extracting sensitivities, independent of the size of the mechanism considered. The sensitivities are non-dimensionalised as,

$$S = \frac{\mathrm{d}\mathcal{J}}{\mathrm{d}g}\frac{g}{\mathcal{J}}, \qquad (11)$$

and normalized by the maximum absolute value of S. For this analysis, the initial mass fractions are $Y_{CH_4} = 0.05$ and $Y_{O_2} = 0.2$ and $Y_{N_2} = 0.75$. The initial temperature is set at $T = 1000\,\text{K}$ in atmospheric pressure as stated in [18]. The extracted sensitivities agree well, and confirm that the reaction $2CH_3(+M) \Rightarrow C_2H_6(+M)$ dominates the ignition process, as far as the Arrhenius parameters are concerned. These results are consistent with those reported in the literature [18].

2.2. Active Subspace Method (ASM)

This section highlights how the aforementioned adjoint-based sensitivity computation is leveraged to
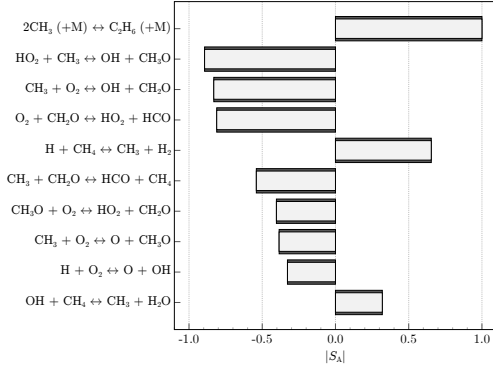
3

Fig. 1: Sensitivity analysis of ignition delay time with respect to A for the ten most dominant reactions using AD (light gray) and CSD (dark gray) for GRI 3.0 mechanism.

perform uncertainty quantification of IDT with respect to the parameters of interest (kinetics, thermodynamics, initial conditions) using the active subspace methodology [9].

The dimension of the parameters space is denoted as D, and the random input variables as $\mathbf{x} = (x_1, \cdots, x_D)$. The distribution of x_j ($j \in [\![1, D]\!]$) is normalised and centered, which may be assumed to be lognormal, uniform, etc. for each parameter. The QoI will be denoted by f. The number of samples M is proportional to the number of the dimensions of the input space D and a factor η.

The active subspace methodology aims to construct an R-dimensional subspace of the D-dimensional parameter space ($R \ll D$) that describes most of the variation of quantity of interest f. The low-dimensional approximation of f is

$$f(\mathbf{x}) \approx G(\mathbf{y}), \quad \mathbf{y} = \mathbf{S}^\top \mathbf{x} \qquad (12)$$

where $G(\mathbf{y})$ is the response surface as, $\mathbf{y} \in \mathbb{K}^R$, $\mathbf{x} \in \mathbb{K}^D$, and $\mathbf{S}$ is an orthogonal matrix ($\mathbb{K} = \mathbb{R}$ or $\mathbb{C}$). The active subspace is then defined as span ($\mathbf{S}$). One way to identify the active subspace is to perform an eigenvalue decomposition of the expectation matrix $\mathbf{C}$ defined as,

$$\mathbf{C} = \frac{1}{M} \sum_{i=1}^{M} \left(\frac{\mathrm{d}f}{\mathrm{d}\mathbf{x}_i} \right) \left(\frac{\mathrm{d}f}{\mathrm{d}\mathbf{x}_i} \right)^\top = \mathbf{W}\mathbf{\Lambda}\mathbf{W}^\top \quad (13)$$

where M denotes the number of samples, $\mathbf{W}$ and $\mathbf{\Lambda}$ the eigenvalues and eigenvectors. Selecting the first R eigenvectors of this decomposition selects the R most dominant directions of the parameter space and provides an approximation of $\mathbf{S} \equiv [\mathbf{w}_1, \cdots, \mathbf{w}_R]$. The motivation for computing the gradients of f at each sample $\mathbf{x}_i$ ($i \in [\![1, M]\!]$) using the adjoint method stems from the fact that it results in the computation of $\mathbf{C}$ scaling as $\ln(D)$ as opposed to $D \ln(D)$ using finite differences.

The error in the estimated eigenvalues and eigenvectors due to an insufficient number of runs can be estimated with bootstrapping [7, 9]. Once the active subspace is identified, various methods, including polynomial fitting, Polynomial Chaos Expansion (PCE) [1, 21] and High Dimensional Model Representation (HDMR) [6], can be employed to construct the response surface. Here a multi-dimensional least-square method is used. A brief summary of the major steps is presented in Tab. 1.

2.3. Linear Approximation using the Adjoint Method (LAAM)

Linear approximation using the adjoint method (LAAM) is proposed here as a low-cost alternative to the active subspace method and is based on linearly approximating the QoI with respect to its input parameter space [22]. While very efficient, it should be noted that for functions with a high degree of non-linearity with respect to the parameter space, this assumption becomes inefficient, an example of this is discussed in Sec. [3.3]. The expansion is performed around the mean of the collected samples, denoted $\overline{\mathbf{x}}$ (the center of the mass), and expressed as

$$\mathrm{QoI}(\mathbf{x}) \equiv f_{LAAM}(\mathbf{x}) \approx \mathrm{QoI}(\overline{\mathbf{x}}) + \left.\frac{\mathrm{dQoI}}{\mathrm{d}\mathbf{x}}\right|_{\overline{\mathbf{x}}} (\mathbf{x} - \overline{\mathbf{x}}).$$
$$(14)$$

Focusing on ignition delay time ($\mathrm{QoI} = \mathrm{IDT}$), the gradient computation is performed using

$$\forall j \in [\![1, N_r]\!], \quad \left.\frac{\mathrm{dIDT}}{\mathrm{d}x_j}\right|_{\overline{\mathbf{x}}} =$$
$$\left.\frac{\mathrm{d}\mathcal{J}}{\mathrm{d}A_j}\right|_{\overline{\mathbf{x}}} A_j(\overline{x}_j) \frac{\ln(UF_j)}{3} \frac{\mathrm{IDT}}{\mathcal{J}} \left(\frac{t_r}{\mathrm{IDT}}\right)^3 \quad (15)$$

where $\mathcal{J}$ and t_r are defined in Eqs. 5 and 6, and $\left(\frac{t_r}{f}\right)^3$ is a normalization factor due to the difference between $\mathcal{J}$ and f. The main advantage of LAAM is that it can provide a good approximation of the uncertainties with only a single function evaluation, regardless of the size of the system. This huge reduction in the computational cost allows rapid analysis of large mechanisms, which will be highlighted in Sec. [3].
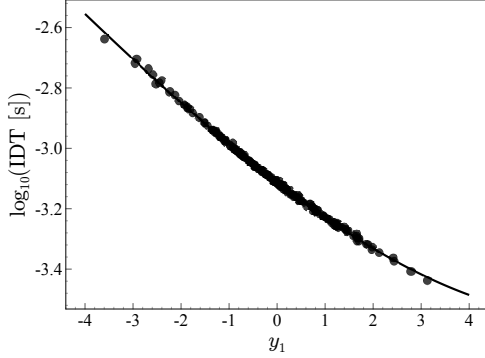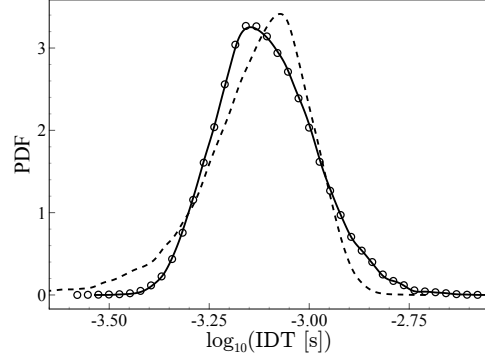
3. Results

In this section, the system uncertainties are first extracted using ASM and LAAM for a range of mechanisms using a single active dimension. A case is then presented where a single dominant direction does not emerge from the eigenmode expansion, motivating the development of a surface reconstruction that relies on a higher-dimensional subspace. Finally, uncertainties with respect to initial conditions are considered to highlight the limitations of the LAAM approach.

3.1. One-dimensional subspace

ASM is used here to construct a response surface for kinetic model parameters. Due to comparatively large available data on hydrogen mechanism ($h2vb$), specifically uncertainty factors and distribution, this

Table 1: Response surface construction algorithm.

1	Choose the appropriate distribution for input variables
2	Assemble M random points of the input space, where $M = \eta \ln (D)$
3	Use adjoint-based method to compute the expectation matrix $\mathbf{C}$ (Eq. 13)
4	Apply eigenvalue decomposition to matrix C and choose the dominant eigenvalues and eigenvectors
5	Estimate upper and lower bounds for the eigenvalues with bootstrapping (vary M and repeat 3 and 4)
6	Construct the mapping matrix $\mathbf{S}$ from the dominant eigenvectors and compute the new variable $\mathbf{y} = \mathbf{S}^{\top}\mathbf{x}$
7	Construct the response surface $G(\mathbf{y}) \approx f(\mathbf{x})$ based on the number of active dimensions

Fig. 2: Comparison of the response surface fitted against a single active direction: •, samples; ——, third degree polynomial fit.

Fig. 3: Comparison of the reconstructed PDF for $h2vb$ mechanism: ——, ASM; ○, Monte Carlo; − − −, LAAM.

mechanism is first employed to benchmark the presented methodologies. Assuming constant temperature, the uncertainties with respect to the reaction rates are mainly attributed to the pre-exponential factors, (A_j), $j \in [\![1, N_r]\!]$ [23]. Following documented studies [14], the random variables (A_j) are assumed to follow a lognormal distribution,

$$\ln (A_j) \sim \mathcal{N} \left\{ \ln \left(A_j^0 \right), \left[\frac{1}{3} \ln (UF_j) \right]^2 \right\}, \quad (16)$$

which are centered and normalised as

$$x_j = \left(\frac{1}{3} \ln (UF_j) \right)^{-1} \ln \left(\frac{A_j}{A_j^0} \right) \sim \mathcal{N}(0,1) \quad (17)$$

where A_j^0 is the mean value of the parameter (the value originally stated by the mechanism) and UF_j is the temperature-independent Uncertainty Factor [24]. The number of input parameters x_i is dependent on the number of elemental reactions. The initial conditions are $Y_{H_2} = 0.29$, $Y_{O_2} = 0.15$, $Y_{N_2} = 0.56$, $T_0 = 1000 \, \text{K}$, and $P_0 = 1.59 \times 10^5 \, \text{Pa}$. Using the normal distribution (Eq. 17), M samples are selected and the value of IDT ($f(\mathbf{x})$) is computed. The gradients are evaluated using the adjoint methodology with J (Eq. 5) as QoI. The extracted gradients are then normalised as

$$\frac{\mathrm{d}f}{\mathrm{d}x_j} = \frac{A_j f}{3\mathcal{J}} \frac{\mathrm{d}\mathcal{J}}{\mathrm{d}A_j} \ln UF_j. \quad (18)$$

As highlighted in Tab. 1, the matrix $\mathbf{C}$ is then constructed and an eigenvalue decomposition is performed to identify the eigenvalues and vectors, before performing bootstrapping to estimate the error bounds. In this particular case $M = 65$ ($\eta = 50$ and $N_{\text{boot}} = 50$) suffices to identify the active direction. There is a difference of about four orders of magnitude between the first and second eigenvalue ($\lambda_1/\lambda_2 \approx 1 \times 10^4$), and a single direction is expected to adequately capture the response surface and the relation between IDT and the (A_j).

Fig. 2 shows a cubic fit between IDT and the reduced space variable y,

$$G(y) = \sum_{n=0}^{3} c_n y^n, \quad (19)$$

where $y = \mathbf{w}_1^{\top}\mathbf{x}$. The values of $c_0 = -3.1144$, $c_1 = -1.2182 \times 10^{-1}$, $c_2 = 6.8 \times 10^{-3}$ and $c_3 = 2.929 \times 10^{-5}$ are computed using the least square method. The resulting probability density function (PDF) using the active subspace strategy is then compared to an application of the Monte Carlo method using $N = 20000$ samples (Fig. 3). The two PDFs match well, and show the mean, μ, and the standard deviation, σ, of around -3.1 and 0.12, respectively. This comparison confirms the adequacy of the QoI used for adjoint estimation for computing the required gradients using ASM method. In order to assess the applicability of LAAM, Fig. 4 compares the linear approximation of IDT to the original function, using the mean extracted from averag-
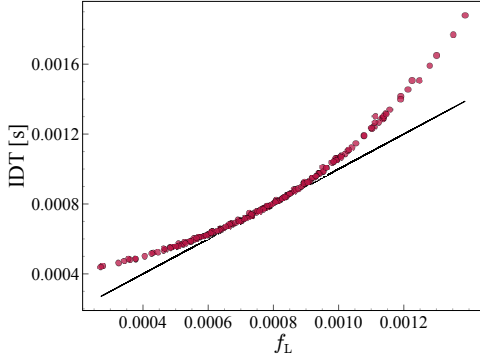
5

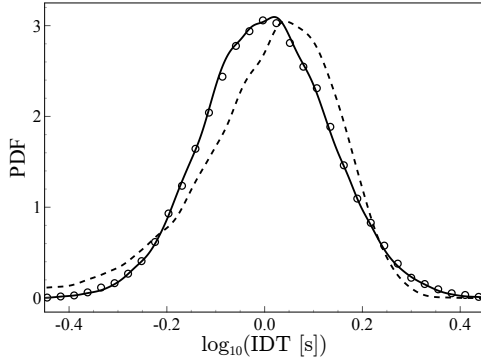Fig. 4: IDT: ——, linear approximation; •, original.

Fig. 5: Comparison of the reconstructed PDF for GRI 3.0 mechanism: ——, ASM; ○, Monte Carlo; $- - -$, LAAM.

Fig. 6: Comparison between different PDFs: ○, Monte Carlo; $...$, response surface using a single eigenvector; $\cdots \times \cdots$, response surface using two eigenvectors; ——, LAAM.

then-backward sweep. The computational expense of ASM compared to LAAM increases significantly as the size of the mechanism increases. This remarkable reduction in cost highlights LAAM's advantage, specifically as a first estimation of the uncertainties of large mechanisms. For demonstration, the cost of the two algorithms are compared in Tab. 2 for various mechanisms using the same number of samples, N. This table confirms that the computational cost of LAAM is negligible compared to ASM, scaling as $\mathcal{O}(\text{N})$.

3.2. Multi-dimensional subspace

The cases that are studied in applications of interest to this work [13, 14] are commonly reduced to a single dominant direction (one dominant eigenvalue), which can be fitted with a response line. However, this can not be generalized to all the operating points, especially when considering uncertainties of IDT, for example in high-density isochoric reactors where the ignition delay time increases.

One such case is replicated here by using similar initial conditions as in [13], for $h2vb$, with a slightly lower initial temperature, $T_0 = 925\,\text{K}$ and mixture composition ($Y_{\text{H}_2} = 0.29$, $Y_{\text{O}_2} = 0.15$, $Y_{\text{N}_2} = 0.56$ and $P_0 = 1.59 \times 10^5\,\text{Pa}$. It should be noted that this case results in higher density compared to the case studied in Sec. [3.1]. As density increases so does IDT and the dispersion of the sample points, causing a polynomial fit using a single dominant direction to become inaccurate, as shown in Fig. 6 where the PDF using a single direction is compared to the Monte Carlo. This figure shows that using a single direction causes the peak to be overpredicted.

However, this issue can be overcome by applying multi-dimensional subspace using the first two eigenvectors. Fig. 7 shows that the majority of the sample points align in a flat surface, which can be mapped using a multi-dimensional least square method fitted to a plane. Comparing the two PDFs in Fig. 6 plotted using 20000 samples exhibits an improvement in

ing $N = 200$ samples. Due to the presence of non-linearities, the linear approximation of IDT deviates from $\mu_{IDT} \pm 2 \times \sigma$. Nevertheless, in this case, due to a small variance of the PDF that clusters the samples around the mean, the linear approximation is found satisfactory. The resulting PDF is compared to that of the Monte Carlo and ASM for $N = 20000$ samples in Fig. 3. The comparison between LAAM and ASM PDFs shows a deviation in the mean by $\epsilon_\mu \approx 10\,\%$ while the error in the variance is $\epsilon_\sigma \approx 2\,\%$. The departure between the peak values of the PDFs is of order $3\,\%$. As a result, the overall approximation of the PDF using LAAM is satisfactory. In order to demonstrate the applicability of the approach to large mechanisms, uncertainties of the kinetic rates for the GRI 3.0 mechanism are extracted and shown in Fig 5. The number of samples used to construct each PDF is $N = 20000$, showing a comparable results to Fig 3. The error in the mean between LAAM and ASM for GRI 3.0 is $\epsilon_\mu \approx 1\,\%$ while the error in the variance is $\epsilon_\sigma \approx 1\,\%$. Due to the similarity in the results produced by the two mechanisms, the imminent analysis will be carried out for $h2vb$ only.

In general, the cost of LAAM is approximately two orders of magnitude lower than ASM, since all the information is gathered using a single forward-
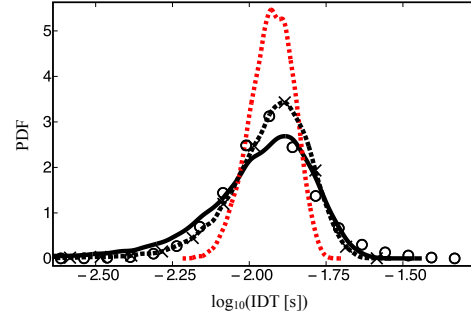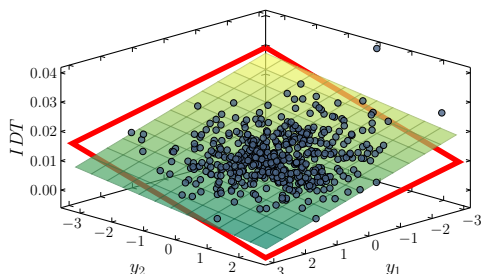
Table 2: Response surface construction algorithm.

Mechanism	h2vb	GRI 1.2	GRI 2.11	GRI 3.0	ITV
Species number	10	32	49	53	490
Reaction number	21	177	297	325	2072
Time$_{LAAM}$ [s]	161.163×10^{-3}	2.57	5.963	14.869	2267.604
Time$_{ASM}$ [s]	50.436	1202.813	3715.522	11570.595	2.683×10^6

Fig. 7: Response surfaces constructed in multi-dimensions : □, LAAM; □ ASM; ●, samples.

Fig. 8: First two dominant eigenvectors, showing the linear combination of rate parameters.

the accuracy using two dominant directions instead of one. Although the three PDFs have similar shapes, the standard deviation of the PDF constructed using a single eigenvector is much lower than the PDFs using Monte Carlo and two eigenvectors. However, it is important to note, that similar to the case considered in the previous section, the deviation in the mean value is not high, therefore we would expect LAAM to also perform satisfactorily in this context.

Fig. 6 also compares the prediction of LAAM to the Monte Carlo, and response surfaces using one and two directions. While similar to the response surface using a single direction the peak of the PDF is not estimated correctly, LAAM is able to predict a correct shape for the distribution. The linear approximation of the QoI using LAAM (Eq. 14) can also be projected on the active directions (y_1, y_2) to assess how well it approximates the response surface. This projection $f_{LAAM}(\mathbf{x}) \Rightarrow f_{LAAM}(y_1, y_2)$ is shown by the plane with the highlighted borders in Fig. 7. This figure shows that LAAM is able to approximate this response surface closely and therefore provides a better approximation than the response surface with only one direction. However, the peak of the PDF is underestimated due to the linearity of the approximation. In order to provide some insight into the manner by which the active dimensions are selected, Fig. 8 shows the linear combination of the rate parameters constructing these dimensions. Comparing the two dominant eigenvectors shows R1 to be the most sensitive reaction in one direction and R5 in the other. Therefore, further analysis is required in order to identify the reaction with the highest overall sensitivity. In multiple directions, the linear combination alone might be misleading and the analysis of the global sensitivity is necessary to understand the reaction pathway. Here, we compute this quantity by cal-
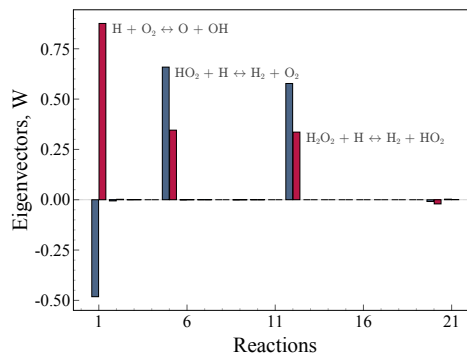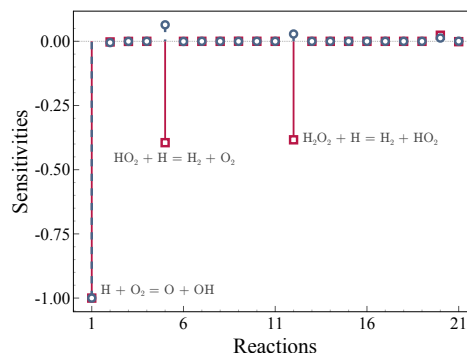

Fig. 9: Global sensitivity of IDT: (red), one active dimension; (blue), two active dimensions.

culating the gradient of the response surface, $\frac{dG(y)}{dx}$, and averaging the result over the entire sample, resulting in the final global gradient with respect to system parameters, as shown in Fig. 9. This figure shows that considering only a single active dimension overestimates the role (sensitivity) of the fifth and twelfth reactions (R5, R12) causing them to have a significant contribution to the ignition process, while using two active dimensions retrieves the dominance of R1 $(H + O_2 = O + OH)$, responsible for OH production, in agreement with the literature [18].

3.3. Initial conditions effect

The results presented in Sec. [3.1] and [3.2] compare the extracted sensitivities using ASM and LAAM for cases exhibiting weakly nonlinear dependence of the QoI with respect to the parameter space. Here, we aim to lift this constraint by extracting
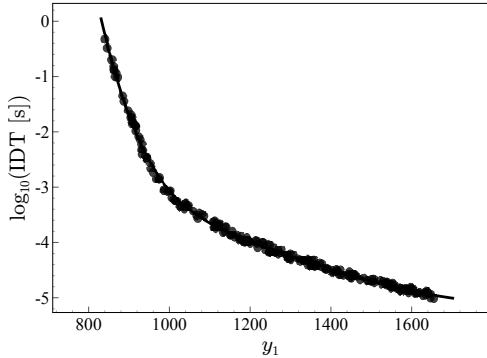
Fig. 10: Comparison of the response surface fitted against a single active direction: •, samples; ——, tenth order polynomial fit.

Fig. 11: Comparison of the reconstructed PDF: ——, ASM; ○, Monte Carlo; − − −, LAAM.

the uncertainties of IDT with respect to variations in the initial conditions, showing strong nonlinear behaviour, and test whether the LAAM approach can provide acceptable predictions.   For this purpose, a random combination of initial fuel mass fraction Y_{0,H_2} to air mass fraction Y_{0,O_2} ratio, and temperature T_0 are extracted from a uniform distribution defined as,

$$\Omega_i = U\big(\Omega_j \times (B+1), \Omega_j \times (B-1)\big), \quad (20)$$

$$\Omega_j = (Y_{\mathrm{H}_2}, Y_{\mathrm{O}_2}, Y_{\mathrm{O}_2}, T_0), \quad (21)$$

where B is the percentage of deviation from the mean value Ω_i. The test case mean value Ω_j will be similar to the studied case in Sec. [3.1] with twenty percent of variation $B = 0.2$ around this value.

Following the procedure for constructing the active subspace, the resulting response surface (not shown here) is divided into two regions, separating igniting and non-igniting samples. Since quantifying the uncertainties of IDT is the purpose of this work, the cases without ignition are discarded, allowing the reduction of the active dimensions to one, as shown in Fig. 10.

The response line is calculated using a tenth-order polynomial. Examining the chosen eigenvector (identified direction) shows that the temperature T_0 has the biggest influence on the selected direction. This can be expected as the temperature affects the reaction rate non-linearly and can cause larger gradients when constructing the expectation matrix, $\mathbf{C}$. Therefore, the uncertainties in IDT are mainly due to the variation in the initial temperature.

The resulting PDFs are shown in Fig. 11. This figure shows that using the response surface in a single direction approximates the overall PDF accurately. The comparison to the PDF built using the LAAM approach shows a large deviation from the rest. This case highlights the limitations of the LAAM approach. Several reasons contribute to this huge deviation between LAAM and Monte Carlo PDFs, but the main factor can be attributed to the use of uniform
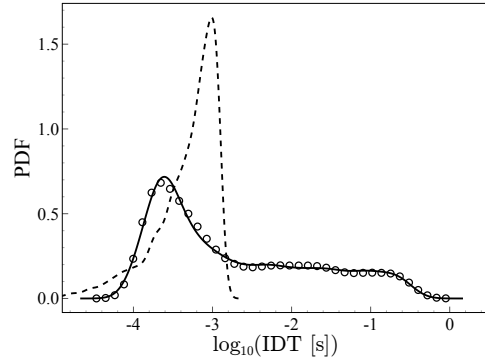
distribution in the presence of a large variance, reducing the correlation between the computed gradient at the mean and the other samples. In addition, at high initial temperatures (above the mean value) the reaction time t_r is very small. As the initial temperature decreases, t_r dramatically increases, causing the deviation in IDT to also increase, resulting in a large tail in the PDF. As a result, the skewness and flatness of the PDF in Fig. 11 are different from the PDFs in Figs. 3 and 6. The resulting PDF is therefore hard to capture using linear approximation. This also necessitates a higher-order polynomial fit (tenth order) when using the ASM method to create the response surface.

However, this error can be reduced by using piecewise linear approximations by splitting the domain into smaller segments and applying LAAM at the mean value of the samples at each part individually [22], or by using higher-order derivatives, which will be the subject of future work.

4. Conclusion and discussion

This study provides a framework for investigating the uncertainties of chemical kinetic models in an isochoric adiabatic reactor configuration. The uncertainties are extracted using active subspace methodology (ASM) coupled with the adjoint method to minimize the cost of evaluating the necessary gradients. The results are also compared to the linear adjoint approximation method (LAAM), which provides a very quick estimation of the overall uncertainties.

In a standard low-density case, where a single dominant direction can be selected, the uncertainties extracted using LAAM and ASM compare well with standard Monte Carlo. Although the accuracy of ASM is better than LAAM for this case, LAAM is able to provide a satisfactory result with a fraction of the cost. Different operating conditions, achieved by modifying the initial conditions, may lead to significant differences in the dispersion of the samples and the number of active dimensions. This is shown in a second case where a single active direction does not come out of the eigenmode expansion, motivating

the use of a multi-dimensional subspace to construct the response surface. Despite the underlying locality and linearity assumptions, LAAM still gives a very good approximation for this case. This suggests that LAAM can be used as a preliminary estimation for UQ especially for large systems.

Finally, the effect of strong nonlinearities on the overall uncertainties are considered. The results prove that the prediction of LAAM deteriorates in these conditions. However, this error can be reduced by using piecewise linear approximations by splitting the domain into smaller segments. This will be the subject of future research.

Acknowledgments

References

[1] M. Hantouche, S. M. Sarathy, O. M. Knio, Global sensitivity analysis of n-butanol reaction kinetics using rate rules, Combust. Flame 196 (2018) 452–465.

[2] A. Doostan, H. Owhadi, A non-adapted sparse approximation of pdes with stochastic inputs, J. Comput. Phys. 230 (8) (2011) 3015–3034.

[3] E. Savin, A. Resmini, J. E. Peter, Sparse polynomial surrogates for aerodynamic computations with random inputs, AIAA conference 18 (2016).

[4] C. E. Rasmussen, C. K. I. Williams, Gaussian processes for machine learning., Adaptive computation and machine learning, MIT Press, 2006.

[5] S. G. Davis, A. B. Mhadeshwar, D. G. Vlachos, H. Wang, A new approach to response surface development for detailed gas-phase and surface reaction kinetic model optimization, Int. J. Chem. Kinet. 36 (2004) 94–106.

[6] A. S. Tomlin, E. Agbro, V. Nevrlý, J. Dlabka, M. Vašinek, Evaluation of combustion mechanisms using global uncertainty and sensitivity analyses: a case study for low-temperature dimethylether oxidation, Int. J. Chem. Kinet 46 (2014) 662–682.

[7] S. Li, B. Yang, F. Qi, Accelerate global sensitivity analysis using artificial neural network algorithm: Case studies for combustion kinetic model, Combust. Flame 168 (2016) 53–64.

[8] H. Wang, D. A. Sheen, Combustion kinetic model uncertainty quantification, propagation and minimization, Progress in Energy and Combustion Science 47 (2015) 1–31.

[9] P. G. Constantine, E. Dow, Q. Wang, Active subspace methods in theory and practice: Applications to kriging surfaces, SIAM J. Sci. Comput. 36(4) (2014) A1500–A1524.

[10] A. Saltelli, M. Ratto, T. Andres, F. Campolongo, J. Cariboni, D. Gatelli, M. Saisana, S. Tarantola, Global sensitivity analysis: the primer, Wiley-Interscience (2008).

[11] M. Eldred, J. Burkardt, Comparison of non-intrusive polynomial chaos and stochastic collocation methods for uncertainty quantification, AIAA J. 2009 (2009) 976.

[12] D. Xiu, J. S. Hesthaven, High-order collocation methods for differential equations with random inputs, SIAM J. Sci. Comput. 27(3) (2005) 1118–1139.

[13] W. Ji, Z. Ren, Y. Marzouk, C. K. Law, Quantifying kinetic uncertainty in turbulent combustion simulations using active subspaces, P. Combust. Inst. 37(2) (2019) 2175–2182.

[14] W. Ji, J. Wang, O. Zahm, Y. M. Marzouk, B. Yang, Z. Ren, C. K. Law, Shared low-dimensional subspaces for propagating kinetic uncertainty to multiple outputs, Combust. Flame 190 (2018) 146–157.

[15] X. Su, W. Ji, Z. Ren, Uncertainty analysis in mechanism reduction via active subspace and transition state analyses, Combust. Flame 227 (2021) 135–146.

[16] A. Hassan, T. Sayadi, V. Le Chenadec, H. Pitsch, A. Attili, Adjoint-based sensitivity analysis of steady char burnout, Combust. Theor. Model. 25 (1) (2021) 96–120.

[17] M. B. Giles, N. A. Pierce, An introduction to the adjoint approach to design, Flow Turb. Combust. 65 (3) (2000) 393–415.

[18] M. Lemke, L. Cai, J. Reiss, H. Pitsch, J. Sesterhenn, Adjoint-based sensitivity analysis of quantities of interest of complex combustion models, Combust. Theor. Model. 47 (2018) 180–196.

[19] F. Schäfer, M. Tarek, L. White, C. Rackauckas, Abstractdifferentiation.jl: Backend-agnostic differentiable programming in julia (2021).

[20] J. J. A. J.J Martins, P. Sturdza, The complex-step derivative approximation, ACM Transactions on Mathematical Software 29 (2003) 245.

[21] P. R. Conrad, Y. M. Marzouk, Adaptive smolyak pseudospectral approximations, SIAM J. Sci. Comput 35 (2013) A2643–A2670.

[22] Q. Wang, K. Duraisamy, J. J. Alonso, G. Iaccarino, Risk assessment of scramjet unstart using adjoint-based sampling methods, AIAA J. 50 (3) (2012) 581–592.

[23] B. D. Phenix, J. L. Dinaro, M. A. Tatang, J. W. Tester, J. B. Howard, G. J. McRae, Incorporation of parametric uncertainty into complex kinetic mechanisms: application to hydrogen oxidation in super-critical water, Combust. Flame 112 (1998) 132–146.

[24] A. A. Konnov, Remaining uncertainties in the kinetic mechanism of hydrogen combustion, Combust. Flame 152 (2008) 507–528.